Sun et al. *Zool. Res.* 2023, 44(5): 905−918
https://doi.org/10.24272/j.issn.2095-8137.2023.106

ZR | Zoological Research

Article Open Access

Choline dehydrogenase interacts with SQSTM1 to activate mitophagy and promote coelomocyte survival in *Apostichopus japonicus* following *Vibrio splendidus* infection

Lian-Lian Sun[1], Ying-Fen Dai[1], Mei-Xiang You[1], Cheng-Hua Li[1,2,*]

[1] *State Key Laboratory for Managing Biotic and Chemical Threats to the Quality and Safety of Agro-products*, *Ningbo University*, *Ningbo*, *Zhejiang* 315211, *China*

[2] *Laboratory for Marine Fisheries Science and Food Production Processes*, *Qingdao National Laboratory for Marine Science and Technology*, *Qingdao*, *Shandong* 266071, *China*

ABSTRACT

Previous studies have shown that *Vibrio splendidus* infection causes mitochondrial damage in *Apostichopus japonicus* coelomocytes, leading to the production of excessive reactive oxygen species (ROS) and irreversible apoptotic cell death. Emerging evidence suggests that mitochondrial autophagy (mitophagy) is the most effective method for eliminating damaged mitochondria and ROS, with choline dehydrogenase (CHDH) identified as a novel mitophagy receptor that can recognize non-ubiquitin damage signals and microtubule-associated protein 1 light chain 3 (LC3) in vertebrates. However, the functional role of CHDH in invertebrates is largely unknown. In this study, we observed a significant increase in the mRNA and protein expression levels of *A. japonicus* CHDH (AjCHDH) in response to *V. splendidus* infection and lipopolysaccharide (LPS) challenge, consistent with changes in mitophagy under the same conditions. Notably, AjCHDH was localized to the mitochondria rather than the cytosol following *V. splendidus* infection. Moreover, *AjCHDH* knockdown using siRNA transfection significantly reduced mitophagy levels, as observed through transmission electron microscopy and confocal microscopy. Further investigation into the molecular mechanisms underlying CHDH-regulated mitophagy showed that AjCHDH lacked an LC3-interacting region (LIR) for direct binding to LC3 but possessed a FB1 structural domain that binds to SQSTM1. The interaction between AjCHDH and SQSTM1 was further confirmed by immunoprecipitation analysis. Furthermore, laser confocal microscopy indicated that SQSTM1 and LC3 were recruited by AjCHDH in coelomocytes and HEK293T cells. In contrast, *AjCHDH* interference hindered SQSTM1 and LC3 recruitment to the mitochondria, a critical step in damaged mitochondrial degradation. Thus, *AjCHDH* interference led to a significant increase in both mitochondrial and intracellular ROS, followed by increased apoptosis and decreased coelomocyte survival. Collectively, these findings indicate that AjCHDH-mediated mitophagy plays a crucial role in coelomocyte survival in *A. japonicus* following *V. splendidus* infection.

Keywords: Choline dehydrogenase; Mitophagy; SQSTM1; Microtubule-associated protein 1 light chain 3; *Apostichopus japonicus*

INTRODUCTION

Mitochondria play a crucial role in intracellular metabolism by producing energy for eukaryotic survival (Nunnari & Suomalainen, 2012). Recent evidence suggests that innate immune cells undergo metabolic reprogramming, and mitochondria are repurposed to produce higher levels of reactive oxygen species (ROS) to promote inflammation and eliminate bacteria following pathogenic invasion (Deng et al., 2008; Liu et al., 2010; West et al., 2011). However, an increasing number of studies have shown that excessive generation of ROS can disrupt redox homeostasis, leading to oxidative stress and damage to cellular and mitochondrial macromolecules (Howard et al., 2002; Luo et al., 2020). Moreover, excessive ROS production can impair mitochondrial metabolic functions and initiate apoptosis, jeopardizing the survival of cells (Youle & Van Der Bliek, 2012). Mitochondria are a major source of cellular ROS, and prolonged excessive ROS production can lead to mitochondrial damage, forming a vicious cycle that ultimately induces cell death, tissue injury, and disease (Barnham et al., 2004). While a series of antioxidant systems preserve the balance between oxidation

Received: 21 May 2023; Accepted: 14 August 2023; Online: 14 August 2023

Foundation items: This work was supported by the National Natural Science Foundation of China (32102825) and Natural Science Foundation of Zhejiang Province (LQ22C190003)

*Corresponding author, E-mail: lichenghua@nbu.edu.cn

and antioxidation, they may not be sufficient to counteract massive ROS accumulation (Apel & Hirt, 2004). In cases where cellular antioxidant systems fail to clear accumulated ROS, the elimination of dysfunctional mitochondria responsible for the generation of these deleterious ROS may be the most effective way to scavenge ROS and maintain cellular redox homeostasis.

Autophagic machinery is involved in the elimination of damaged mitochondria and related ROS through a process known as mitochondrial autophagy (mitophagy), which plays a crucial role in the immune response to bacterial infections (Ding et al., 2010). Numerous studies have revealed that elevated ROS can trigger mitophagy (Volpe et al., 2018; Zeb et al., 2021). The degradation of dysfunctional mitochondria through mitophagy is a complex process involving the coordination of autophagic machinery with adaptors and receptors located in the outer mitochondrial membrane (Yamano et al., 2016). Thus, adaptors and receptors play a crucial role in initiating mitophagy by linking damaged mitochondria with LC3, a marker protein for autophagy. The most common adapters, such as SQSTM1/p62, OPTN, TAX1BP1/T6BP, NDP52, and NBR1 (neighbor of BRCA1 gene 1), have the ability to link LC3 and PINK1/Parkin ubiquitinated mitochondria in a bispecific manner (Nguyen et al., 2016; Yoo & Jung, 2018). In contrast, other receptors, such as FUNDC1, BNIP3, and NIX/BNIP3L, can directly interact with LC3, thus facilitating the linkage of phagophores with targeted mitochondria and the initiation of mitophagy (Liu et al., 2014; Yoo & Jung, 2018). Recent studies have identified a novel mitochondrial receptor, choline dehydrogenase (CHDH), which can simultaneously recognize non-ubiquitinated damaged mitochondria and LC3 (Yoo & Jung, 2018).

CHDH, an essential enzyme localized on the matrix side of the mitochondrial inner membrane, catalyzes the oxidation of choline to betaine aldehyde, a necessary process for acetylcholine production (De Ridder & Van Dam, 1973). Initially isolated from rat liver mitochondria, CHDH exhibited enzymatic activity only when its two functional domains, flavin adenine dinucleotide (FAD) and iron sulfur cluster, were appropriately assembled (Lin & Wu, 1986). CHDH also plays a crucial role in activating mitophagy, an autophagic process that selectively targets damaged mitochondria (Park et al., 2014). Up-regulation of CHDH can accelerate CCCP-induced mitophagy and PARK2/parkin-mediated removal of mitochondria, while its down-regulation significantly inhibits both mitophagy and removal of damaged mitochondria in SN4741 dopaminergic neuronal cells and HeLa cells (Park et al., 2014). Intriguingly, Park et al. (2014) also revealed that while CHDH is present in both the inner and outer mitochondrial membranes under normal circumstances, although absent in the cytosol and mitochondrial matrix, it only accumulates in the outer mitochondrial membrane during mitophagy activation. They also proposed a novel mechanism in which CHDH recruits LC3 to the autophagosome through direct interaction with SQSTM1, forming a ternary complex. This complex is then transported to the mitochondria, where it activates the autophagic processes necessary for the degradation and elimination of damaged or infected mitochondria (Park et al., 2014). However, while the mechanism of CHDH-mediated mitophagy in mammals is relatively well understood, further research is needed to explore the physiological significance of mitophagy in invertebrates and determine how CHDH recruits autophagosomes to the mitochondria in these organisms.

Sea cucumbers (*Apostichopus japonicus*), an economically valuable marine species, occupy a unique evolutionary position between invertebrates and vertebrates and rely solely on innate immunity to defend against bacterial infections (Ma et al., 2006). In our previous study on *A. japonicus* defense mechanisms against *Vibrio splendidus* infection, we revealed the pivotal role of coelomocytes in altering mitochondrial metabolism to generate substantial ROS for pathogen elimination, while also showing that *V. splendidus* infection induces mitophagy, contributing to the removal of excessive ROS from coelomocytes (Sun et al., 2020). However, the well-characterized PINK1 and Parkin-driven mitophagy pathway has not been identified in sea cucumbers, necessitating the exploration of alternative mitophagy pathways involving mitochondrial receptors such as CHDH. This mitochondrial receptor can simultaneously recognize non-ubiquitinated damage signals and LC3, making it a promising subject for investigating its regulatory mechanisms in mitophagy. In this study, we first cloned CHDH from *A. japonicus*, analyzed its structural domain characteristics, and investigated the relationship between CHDH and damaged mitochondrial clearance. By exploring the regulatory mechanisms of CHDH in mitophagy, we should gain important insights into the intricate relationship between CHDH expression and coelomocyte survival, thereby shedding light on the potential mechanisms underpinning skin ulceration syndrome in *A. japonicus* from a new perspective.

MATERIALS AND METHODS

Ethics statement

All sea cucumbers (*A. japonicus*) and Institute of Cancer Research (ICR) mice used in the study were commercially cultured animals. All animal study protocols were reviewed and approved by the Animal Ethics Committee of Ningbo University (Permit No.: 10506), and all animals were handled according to the recommendations of the Guide for the Care and Use of Laboratory Animals of the National Institutes of Health.

Experimental animals and *V. splendidus* infection

Healthy sea cucumbers (125±15 g) were obtained from the Dalian Pacific Aquaculture Company (Dalian, China) and acclimated to a constant environment with aerated natural seawater (temperature 16 °C and salinity 29±1) for three days before the experiment. The experimental animals were randomly assigned into five groups, with at least 15 individuals per group. To investigate the effects of CHDH on mitophagy in pathogen-infected *A. japonicus*, four groups were immersed in live *V. splendidus* at a final concentration of 1×10^7 colony forming units (CFU)/mL for 6, 24, 48, and 72 h, while the untreated group served as the control (0 h). After *V. splendidus* treatment, all sea cucumbers were sacrificed, followed by the collection of coelomocytes from three individuals (pooled as one sample), with five replicates for both the control and experimental groups. The coelomic fluids were filtered using a 200 mesh cell cribble to remove other tissue debris, then mixed with ice-cold anticoagulant solution (0.068 mol/L Tri-HCl, 0.019 mol/L KCl, 0.48 mol/L NaCl, and 0.02 mol/L EGTA, pH 7.6) at a 1 : 1 (v : v) ratio. After centrifugation at 800 ×*g* and 16 ℃ for 5 min, the coelomocytes were resuspended in ice-cold isotonic buffer (0.01 mol/L Tri-

HCl, 0.53 mol/L NaCl, and 0.001 mol/L EGTA, pH 7.6) and centrifuged again. The cells were then pulverized into powder using liquid nitrogen and frozen in ultralow temperature refrigerators (−80 °C) for time-course expression analysis at the mRNA and protein levels.

Primary coelomocyte culture and treatment

The protocols for isolating and culturing primary coelomocytes *in vitro* were previously described by Zhang et al. (2014). Coelomic fluids were harvested from healthy *A. japonicus* individuals and mixed with anticoagulant solution at a 1 : 1 (v:v) ratio. The isolated coelomocytes were washed twice through centrifugation in isotonic buffer and resuspended in Leibovitz's L-15 cell culture medium (Invitrogen, USA) supplemented with streptomycin sulfate (100 μg/mL) and penicillin (100 U/mL). The coelomocytes were then inoculated at a density of 1×10^6 cells/well in 24-well culture microplates and cultured for 12 h with serum-free medium at 16 °C. To investigate the function of CHDH in coelomocyte mitophagy, the cells were treated with 10 μg/mL lipopolysaccharide (LPS, Sigma, USA) purified from *Escherichia coli* (055: B5) for 1, 3, 6, 12, and 24 h. After LPS challenge, the cells were collected from four wells as one sample, with three biological replicates performed. Cells without LPS challenge were regarded as the control group.

Cloning and sequence analysis of *A. japonicus* CHDH (AjCHDH)

Total RNA from each sample was extracted using RNAiso Plus (Takara, Japan) following the manufacturer's protocols. RNA quality and quantity were assessed using a NanoDrop 2000. RNA samples with 260/280 and 260/230 ratios greater than 1.8 were reverse-transcribed into cDNA using a PrimeScript RT Reagent Kit with gDNA Eraser (Takara, Japan). To amplify the complete open reading frame (ORF) of *AjCHDH*, primers (listed in Supplementary Table S1) were designed based on expressed sequence tags (ESTs) of *CHDH* obtained from transcription data of *A. japonicus* (Zhang et al., 2014). The purified gene fragments from agarose gels were ligated into the pMD19-T simple vector (Takara, Japan), transformed into competent *E. coli* DH5α cells (Takara, Japan), and sequenced by Sangon Biotech (China). To verify the accuracy and functionality of AjCHDH, the BLAST algorithm and SMART server were used to analyze sequence characteristics, including signal peptides, molecular weight, isoelectric point, and conserved domains. Multiple alignment analysis of AjCHDH and other CHDH species was performed using DNAMAN software to create and annotate sequence differences. Furthermore, a phylogenetic tree was generated using the neighbor-joining method in MEGA v5.1 to reveal the evolutionary relationships between AjCHDH and other CHDH family members, with 1 000 bootstrap replicates.

Quantitative real-time polymerase chain reaction (qRT-PCR)

To explore the changes in relative mRNA levels following pathogen invasion, total RNA was extracted from samples obtained after *V. splendidus* treatment and LPS challenge. The extracted RNA was then reverse-transcribed into single-stranded cDNA using a PrimeScript RT Reagent Kit to remove genomic DNA. Relative mRNA abundance was determined with a 7500 Real-Time PCR System using a SYBR Green Plus Reagent Kit (Takara, Japan) and corresponding primers (listed in Supplementary Table S1). The qRT-PCR conditions were set according to the provided instructions. The relative fold-induction of target mRNAs was calculated using the $2^{-\Delta\Delta CT}$ method, then normalized to the internal control *Ajβ-actin* mRNA abundance (Livak & Schmittgen, 2001).

Recombinant protein expression, polyclonal antibody preparation, and western blot analysis

Specific primers were designed to amplify the complete ORF of *AjCHDH* (Supplementary Table S1). The amplified product containing *Bam*HI and *Not*I restriction sites was inserted into the pET-28a expression vector and transformed into *E. coli* BL21 (DE3). The cells were then induced with isopropyl thiogalactoside (1 mmol/L) to express the His-tagged recombinant protein rAjCHDH, which was purified using His-Trap™ Ni-agarose. To generate polyclonal antibodies against rAjCHDH, four male ICR mice (20 g, 6–8 weeks old) were purchased from Beijing Vital River Laboratory Animal Technology (China) and immunized with purified rAjCHDH protein following previously described methods (Sun et al., 2022). Antiserum was collected from the eyes and stored at ultralow temperatures for further immunoblot analysis. For immunoblotting, coelomocytes treated with *V. splendidus* and LPS were lysed in RIPA buffer containing 100 mmol/L phenylmethylsulfonyl fluoride (PMSF, Beyotime, China). After boiling the samples for 10 min at 100 °C, 50 μg of protein was separated using 15% sodium dodecyl sulfate-polyacrylamide gel electrophoresis (SDS-PAGE) and transferred onto polyvinylidene difluoride (PVDF) membranes. The membranes were then blocked with 5% skim milk and incubated overnight at 4 °C with primary antibodies against rAjCHDH (dilution: 1 : 200), LC3 (dilution: 1 : 1000, AB51520, Abcam, UK), SQSTM1 (dilution: 1 : 1000, A7758, ABclonal, USA), Tim23 (dilution: 1 : 1000, 67535-1-Ig, Proteintech, USA), COX IV (dilution: 1 : 1000, AC610, Beyotime, China), and Ajβ-actin (dilution: 1 : 2000, M20011M, Abmart, China). After washing, the membranes were incubated with horseradish peroxidase (HRP)-conjugated secondary antibodies (Sangon Biotech, China) for 1.5 h at room temperature. Finally, the protein bands were incubated with an enhanced chemiluminescence (ECL) reagent (Bio-Rad, USA) for 1 min and detected using an Omega Lum C imaging system (Aplegen, USA).

Determination of protein levels in mitochondria and cytosol

The mitochondrial and cytosolic fractions of coelomocytes were separately isolated using a Cell Mitochondria Isolation Kit (Beyotime, China) following the provided protocols, as described previously (Bao et al., 2019). Briefly, coelomocytes collected from *A. japonicus* infected with *V. splendidus* for 0, 6, 24, 48, and 72 h were washed twice and incubated in 1.5 mL of mitochondrial lysis buffer for 15 min at 4 °C. After homogenization for 30 strokes, the homogenate was centrifuged at 1 000 ×*g* for 10 min at 4 °C to remove nuclei and unbroken cells. The supernatant was then transferred to another centrifuge tube and centrifuged at 3 500 ×*g* and 4 °C for 10 min, with the sediment being the mitochondria. To obtain the mitochondrial proteins, 150–200 μL of mitochondrial lysate containing 1% PMSF was added to the mitochondrial sample. COX IV was used as an internal control. To obtain the cytosolic protein, the collected supernatant was centrifuged again at 12 000 ×*g* for 10 min at 4 °C to remove the mitochondria. Finally, mitochondrial and cytosolic protein levels were measured using western blot analysis.

Subcellular localization of AjCHDH in coelomocytes

Coelomocytes were inoculated in 6-well plates to investigate

the regulatory relationship between AjCHDH and mitophagy following LPS challenge for 24 h. To stain the mitochondria, MitoTracker Red CMXRos (200 nmol/L) was used to treat the cells for 25 min. After twice rinsing with 1×phosphate-buffered saline (PBS), the coelomocytes were fixed using 4% paraformaldehyde (PFA) in PBS and permeabilized with 0.1% Triton X-100. The cells were then blocked with 5% bovine serum albumin (BSA) and labeled with primary antibodies (anti-AjCHDH, dilution: 1 : 200) at 4 °C overnight. Thereafter, the coelomocytes were washed with 1×PBS three times, incubated with Alexa Fluor 488 conjugated secondary antibodies (Beyotime, China) for 1 h at room temperature, then tagged with 4',6-diamidino-2-phenylindole (DAPI, Beyotime, China) to visualize nuclei. Finally, the colocalization of AjCHDH and mitochondria was analyzed using laser scanning spectral confocal microscopy (TCS SP2, Leica).

AjCHDH interference

Specific small interfering RNAs (siRNAs) targeting *AjCHDH*, as well as the negative control, were obtained from the GenePharma Company (China) (Supplementary Table S1). A total of 1×10^6 coelomocytes were seeded in 24-well plates without serum and transfected with siRNA using Lipofectamine 6000 reagent (Beyotime, China) following the manufacturer's protocols. After exposure to siRNA for 24 and 48 h, the cells were collected to determine the interference efficiency in mRNA and protein expression levels, respectively.

Colocalization of mitochondria and lysosomes

To assess changes in AjCHDH at the mitophagy level, primary coelomocytes were cultured on 24-well plates and transfected with *AjCHDH* siRNA for 24 h. For labeling mitochondria and lysosomes, MitoTracker Green (20–200 nmol/L, Beyotime, China) and LysoTracker Red (50–75 nmol/L, Beyotime, China) were added to the living cells according to the provided instructions. After loading with MitoTracker Green and LysoTracker Red for 1 h, the stained coelomocytes were twice washed with 1×PBS, and the number of orange fluorescent puncta was observed using Leica scanning spectral confocal microscopy.

Transmission electron microscopy (TEM)

The presence of intracellular double-membrane vesicles housing mitochondria, known as mitochondrial autophagosomes, can serve as an important indicator of the level of mitophagy based on the degree of mitochondrial degradation. To determine the necessity of AjCHDH in initiating mitophagy following pathogen infection, we treated coelomocytes cultured in 6-well plates with *AjCHDH* siRNA for 24 h and *V. splendidus* for another 24 h, then observed the changes in mitophagy levels under an electron microscope (H7650, Hitachi, Japan). Briefly, the treated cells were collected and kept in 2.5% glutaraldehyde for over 24 h at 4 °C. After rinsing with PBS (0.1 mol/L, pH 7.4), the post-fixed coelomocytes were exposed to 1% osmium tetroxide for secondary fixation, then dehydrated in graded ethanol concentrations, mixed in anhydrous acetone, embedded in epoxy resin (EMbed-812; Electron Microscopy Sciences, USA), sliced into ultrathin sections, stained with uranyl acetate and lead citrate, and imaged by TEM.

Mitochondrial membrane potential (ΔΨm) assay

Membrane potential serves as a key indicator of mitochondrial health, with injured mitochondria losing this potential, making them targets for scavenging by AjCHDH-driven mitophagy (Elmore et al., 2001). We speculate that the effects of AjCHDH on mitophagy occur via changes in ΔΨm levels. To analyze ΔΨm, primary coelomocytes transfected with *AjCHDH* siRNA were treated with LPS for 24 h and assessed using a JC-1 Assay Kit (Beyotime, China) according to the provided instructions. After coincubation with JC-1 working solution for 25 min at 37 °C, all treated cells were centrifuged for 5 min (800 ×*g*, 4 °C), twice washed with JC-1 buffer solution, and processed for flow cytometry (Becton Dickinson Biosciences, USA), with normal mitochondria producing red fluorescence and depolarized mitochondria producing green fluorescence. The ratio of red/green JC-1 fluorescence intensity was calculated to indicate ΔΨm (Métivier et al., 1998).

Coimmunoprecipitation assay

Park et al. (2014) demonstrated that CHDH accumulation in damaged mitochondria can recruit SQSTM1 and LC3 to induce mitophagy when mitochondria lose membrane potential. To further investigate the role of AjCHDH in the activation of mitophagy, we treated sea cucumbers with *V. splendidus* for 72 h and lysed the coelomocytes to obtain supernatant for immunoprecipitation analysis. The protein from the supernatant was mixed with anti-AjCHDH antibodies (dilution: 1 : 200) at 4 °C with continuous rotation overnight and added to 30 μL of protein A/G beads (Beyotime, China). The immunoprecipitates were then harvested, boiled, and analyzed using western blotting with anti-AjCHDH, anti-LC3, and anti-SQSTM1 antibodies.

Immunofluorescence staining

To perform immunofluorescence staining, coelomocytes cultured in 6-well plates were treated with LPS for 24 h, washed twice with PBS, and fixed with 4% paraformaldehyde for 30 min at room temperature. Subsequently, the cells were incubated with 0.1% Triton X-100 and 5% BSA and co-labeled with a mouse primary antibody for AjCHDH (dilution: 1 : 200), rabbit primary antibody for LC3 (dilution: 1 : 1000), mouse primary antibody for AjCHDH (dilution: 1 : 200), and rabbit primary antibody for SQSTM1 (dilution: 1 : 1000) overnight at 4 °C. The cells were further incubated with corresponding fluorescent secondary antibodies (Alexa Fluor 488-conjugated goat anti-mouse IgG and Cy3-conjugated goat anti-rabbit IgG) for 2.5 h before DAPI staining, with the colocalization of AjCHDH with LC3 and SQSTM1 captured using Leica scanning spectral confocal microscopy.

Colocalization of AjCHDH, SQSTM1, and LC3 in HEK293T cells

To construct expression plasmids, the complete ORFs of AjCHDH, SQSTM1, and LC3 were separately amplified using specific primers (Supplementary Table S1) and ligated into the pCMV-N-mCherry vector (Beyotime, China), pEGFP-N3 vector (Beyotime, China), and pIRES2-EGFP vector (Beyotime, China) according to the instructions of the plasmid vector. Simultaneously, the ORF of SQSTM1 was also ligated into the pCMV-Flag-2C vector to construct the pCMV-Flag-2C-SQSTM1 plasmid. In addition, HEK293T cells were seeded into 6-well plates under 5% CO_2 at 37 °C. Recombinant target plasmids (pCMV-N-mCherry-AjCHDH, pEGFP-N3-SQSTM1, pCMV-N-mCherry-AjCHDH, pCMV-Flag-2C-SQSTM1, and pIRES2-EGFP-LC3) were co-transfected into HEK293T cells using Lipofectamine 6000 following the manufacturer's protocols. After 24 and 36 h of transfection, the HEK293T cells

were twice washed with 1×PBS and stained with DAPI. Finally, the colocalization of AjCHDH with SQSTM1 and LC3 was observed via Leica scanning spectral confocal microscopy.

Measurement of intracellular and mitochondrial ROS

DCFH-DA (2',7'-dichlorofluorescin diacetate) probes were used to detect intracellular ROS after *AjCHDH* interference and LPS treatment for 24 h following the instructions. Briefly, coelomocytes were co-incubated with DCFH-DA probes (10 μmol/L, excitation wavelength: 500 nm, emission wavelength: 525 nm) in 24-well cell culture plates at 37 °C for 30 min and measured by flow cytometry. To confirm the importance of AjCHDH in eliminating mitochondrial ROS, we transfected coelomocytes with *AjCHDH* siRNA, followed by LPS stimulation for 24 h. All treated cells were then stained with MitoSOX Red mitochondrial superoxide indicator (Yeasen, China) and analyzed under a confocal microscope.

Analysis of coelomocyte apoptosis and survival

Damaged mitochondria generate excessive ROS, thereby triggering cell apoptosis and threatening cell survival. Mitophagy is considered the most effective way to remove damaged mitochondria (Tolkovsky, 2009; Youle & Van Der Bliek, 2012). In this study, an Annexin V-FITC Apoptosis Detection Kit (Beyotime, China) was used to determine the influence of AjCHDH-mediated mitophagy on coelomocyte apoptosis. Briefly, coelomocytes were transfected with *AjCHDH* siRNA for 24 h prior to treatment with LPS for 24 h. Subsequently, cells were harvested and incubated with a mixture of Annexin V-FITC and propidium iodide (PI) for 20 min in the dark, with apoptosis then analyzed by flow cytometry following the manufacturer's protocols. In addition, coelomocyte survival was examined using a Cell Proliferation and Cytotoxicity Assay Kit (Beyotime, China). Briefly, 100 μL of coelomocytes were plated in a 96-well plate, transfected with *AjCHDH* siRNA, and treated with LPS for 24 h. Subsequently, 10 μL of MTT reagent was added to the treated cells for 4 h. After the supernatant was discarded, 200 μL of dimethyl sulfoxide (Sigma-Aldrich, USA) was added to the wells, with optical density at 570 nm determined using a microplate reader.

Statistical analysis

All results were obtained based on at least three independent repeated experiments and displayed as means ± standard errors of the mean (*SEMs*) (n=3). To determine significant differences between the control and experimental groups, one-way analysis of variance (ANOVA) with multiple comparisons was used, while Student's t-test was used to evaluate data between two groups. *: P<0.05 and **: P<0.01 indicated significant differences.

RESULTS

AjCHDH accumulated in coelomocyte mitochondria after *V. splendidus* infection and LPS challenge

Previous research has demonstrated that CHDH located on the mitochondrial outer membrane plays a critical role in mitophagy (Park et al., 2014). In this study, we investigated the expression pattern and subcellular localization of AjCHDH in response to pathogenic infection. As shown in Figure 1A, B, we found that AjCHDH expression in coelomocytes increased at the mRNA and protein levels after *V. splendidus* and LPS treatment in a time-dependent manner, suggesting a relationship between AjCHDH expression and pathogenic infection. Compared to the control group, coelomocytes infected with bacteria exhibited a significant increase in *AjCHDH* transcription at 24 and 48 h (4.63-fold (P<0.05) and 6.56-fold (P<0.05), respectively), reaching a peak at 72 h (12.90-fold, P<0.01). Consistently, coelomocytes challenged with LPS showed an up-regulation in *AjCHDH* expression at each time point, with a 6.32-fold (P<0.01) increase observed at 24 h. Subsequently, we investigated the subcellular localization of AjCHDH in coelomocytes after LPS challenge by immunofluorescence staining. Results showed that LPS challenge increased AjCHDH expression and colocalization with mitochondria (Figure 1C), implying that AjCHDH increased and accumulated in mitochondria during mitophagy. Additionally, we assessed the protein expression levels of AjCHDH in the mitochondria and cytosol following *V. splendidus* infection. As illustrated in Figure 1D, E, AjCHDH was predominantly located within the mitochondria, and its expression increased gradually with infection duration.

Involvement of AjCHDH in coelomocyte mitophagy following *V. splendidus* infection *in vivo* and LPS challenge *in vitro*

Mitophagy represents the most efficient mechanism for eliminating impaired mitochondria, and previous research has highlighted the crucial role of CHDH in this process (Park et al., 2014). In the current study, we aimed to determine the necessity of CHDH in regulating mitophagy in *A. japonicus*. Coelomocytes were transfected with *AjCHDH* siRNA, resulting in a significant 50% decrease (P<0.05) in *AjCHDH* mRNA level, accompanied by a corresponding reduction in protein level (Figure 2A). After *AjCHDH* knockdown, the mitophagy level induced by LPS treatment in coelomocytes showed a decrease, as illustrated by the decrease in the colocalization of mitochondria and lysosomes (Figure 2B). Furthermore, TEM observations confirmed that *AjCHDH* interference followed by *V. splendidus* infection significantly inhibited mitophagy and the clearance of damaged mitochondria (Figure 2C). Additionally, the JC-1 staining results demonstrated that *AjCHDH* knockdown blocked the removal of depolarized mitochondria, as indicated by the significant down-regulation in ΔΨm of coelomocytes transfected with *AjCHDH* siRNA (Figure 2D, E).

AjCHDH interacted with SQSTM1 to activate mitophagy

To investigate the mechanism by which AjCHDH regulates mitophagy, we cloned and analyzed its structural domain. The complete ORF of *AjCHDH* (GenBank accession number OQ254783) was 1 803 bp in length, encoding 600 residues (Figure 3A), with a predicted molecular mass of 66.9 kDa and theoretical *pI* of 8.85. SMART analysis revealed that AjCHDH possessed a glucose-methanol-choline (GMC) oxidoreductase domain (52–343 amino acids (aa)) at the N-terminus, a GMC oxidoreductase domain at the C-terminus (435–573 aa), and a signal peptide (1–23 aa) (Figure 3B), which were highly conserved (Supplementary Figures S1, S2). While AjCHDH lacked a structural domain to bind to LC3 directly, it contained a structural domain capable of binding to SQSTM1 (Figure 3B). As SQSTM1 represents an important adaptor for connecting damaged cargo to LC3 (Jin & Youle, 2012; Pankiv et al., 2007), we speculated that AjCHDH can recruit LC3 by interacting with SQSTM1. Therefore, we predicted the

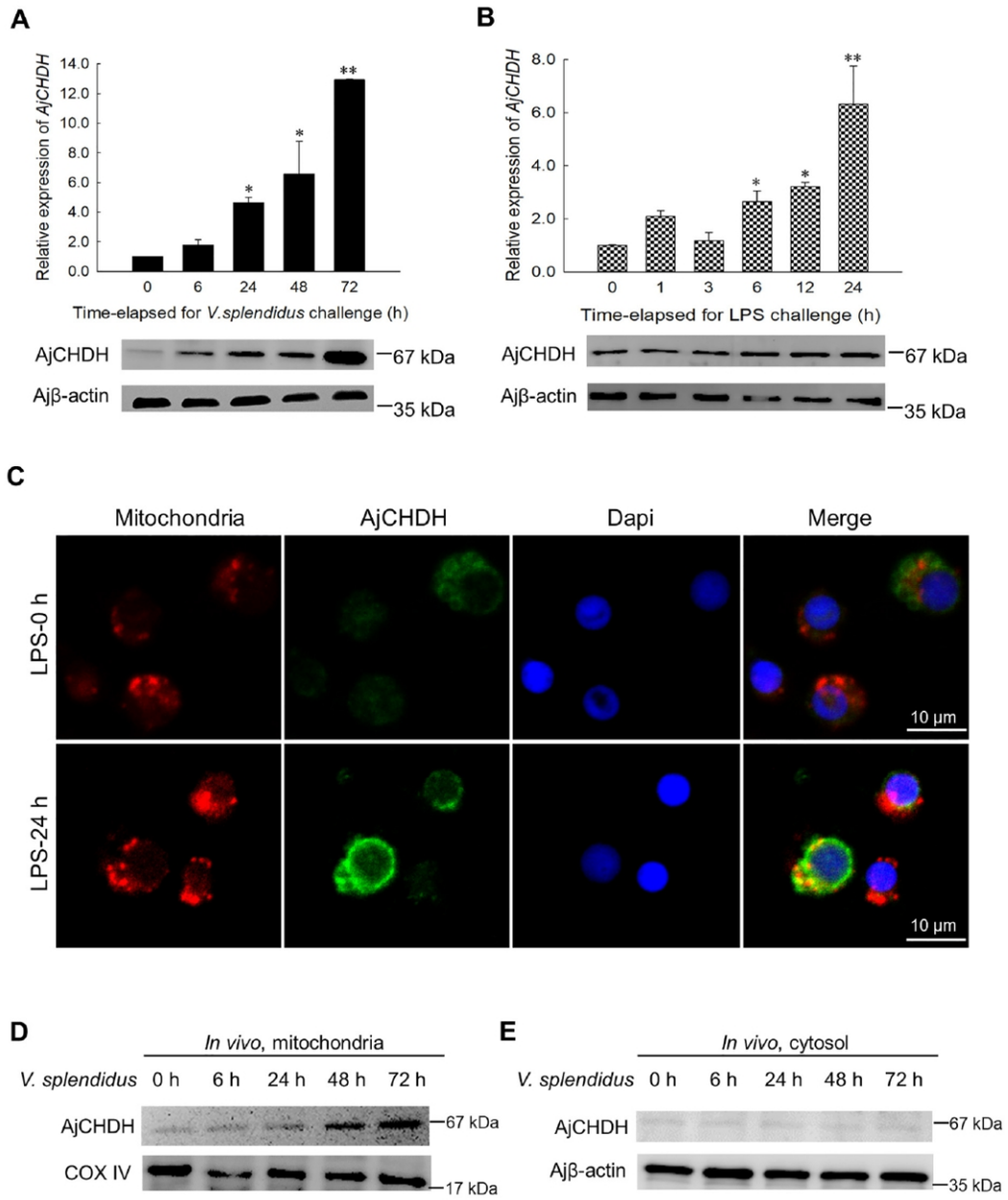

Figure 1 AjCHDH accumulated in mitochondria of coelomocytes after *Vibrio splendidus* infection and LPS challenge

A: Temporal expression analysis of AjCHDH at the mRNA and protein levels in response to *V. splendidus* infection *in vivo*. *: $P<0.05$; **: $P<0.01$, $n=5$. B: Temporal expression analysis of AjCHDH at the mRNA and protein levels in response to LPS challenge *in vitro*. *: $P<0.05$; **: $P<0.01$, $n=3$. C: Immunofluorescence colocalization analysis of AjCHDH with mitochondria in control coelomocytes and LPS-treated cells for 24 h, with DAPI (blue) staining to identify nuclei. D: Expression analysis of AjCHDH in response to *V. splendidus* infection in mitochondria. E: Expression analysis of AjCHDH in response to *V. splendidus* infection in cytosol. CHDH: Choline dehydrogenase; COX IV: Cytochrome c oxidase IV.

combination models of AjCHDH and SQSTM1, as well as SQSTM1 and LC3, using Discovery Studio (Figure 3C, D), which implied that AjCHDH may recruit LC3 and activate mitophagy by interacting with SQSTM1. Indeed, immunoprecipitation verified that AjCHDH interacted with SQSTM1 and LC3 after *V. splendidus* infection for 72 h (Figure 3E, F).

AjCHDH recruited SQSTM1 and LC3 during mitophagy

To gain further insights into the regulatory mechanism of mitophagy mediated by AjCHDH, we investigated the colocalization of AjCHDH with SQSTM1 and LC3 in both control and LPS-treated coelomocytes. Confocal microscopy indicated that AjCHDH colocalized with SQSTM1, as evidenced by the substantial overlap between the two signals at the pixel level after 24 h of LPS challenge (Figure 4A). Consistently, in untreated cells, the presence of orange dots indicating interactions between AjCHDH and LC3 were minimal, although more orange dots were observed after LPS challenge (Figure 4B). To confirm this interaction relationship, we cotransfected HEK293T cells with the constructed pCMV-N-mCherry-AjCHDH and pEGFP-N3-SQSTM1 plasmids. As shown in Figure 4C, AjCHDH colocalized with SQSTM1, and fluorescence-labeled proteins significantly increased after cotransfection for 36 h compared to cells transfected for 24 h. Similarly, coexpression with pCMV-N-mCherry-AjCHDH, pCMV-Flag-2C-SQSTM1, and pIRES2-EGFP-LC3 resulted in

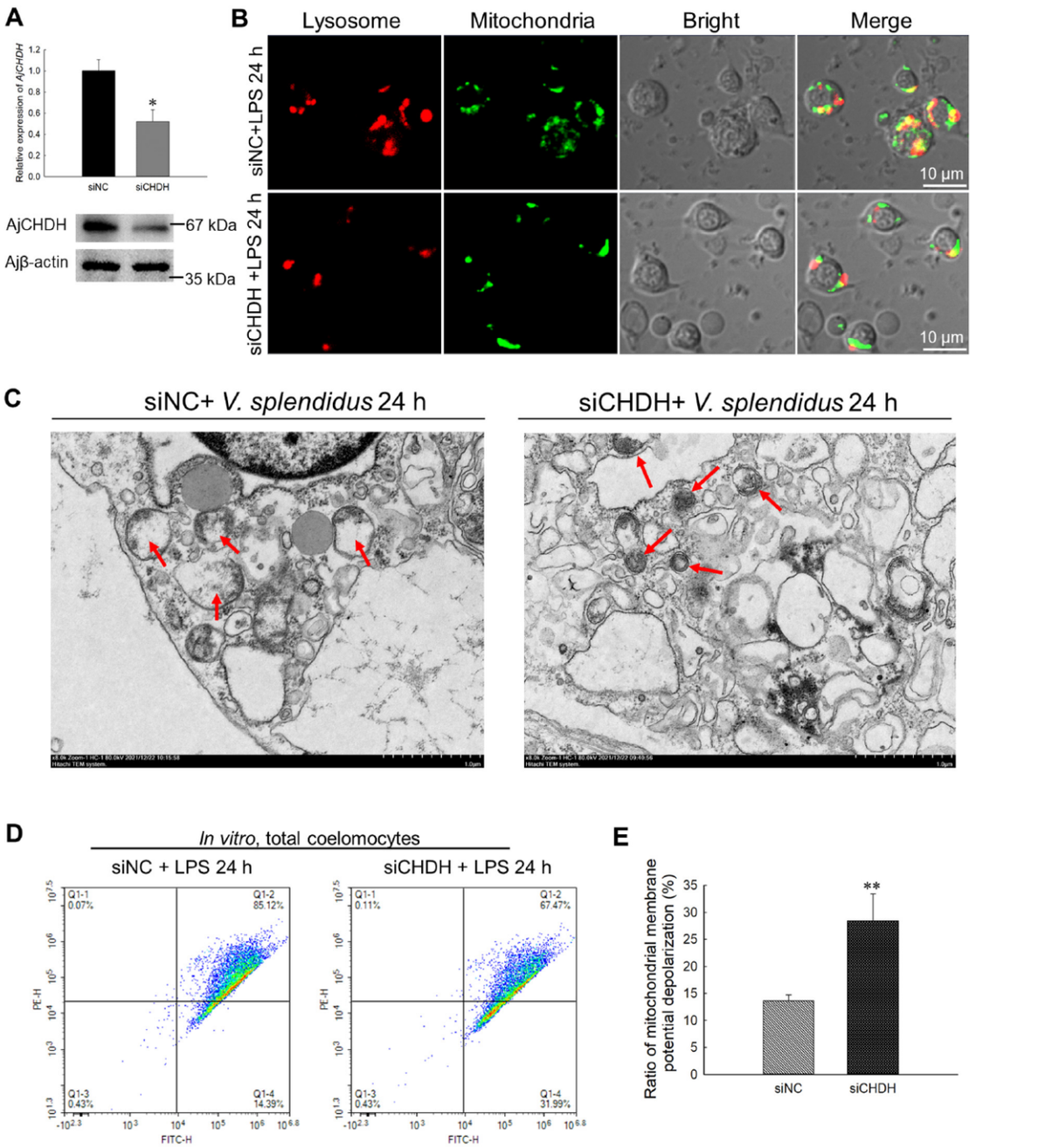

Figure 2 AjCHDH was involved in coelomocyte mitophagy following *Vibrio splendidus* infection *in vivo* and LPS challenge *in vitro*

A: AjCHDH mRNA and protein expression levels in coelomocytes after 24 and 48 h of transfection with or without *AjCHDH* siRNA. *: $P<0.05$; **: $P<0.01$, $n=3$. B: Immunofluorescence colocalization analysis of LysoTracker Red with MitoTracker Green in coelomocytes after *AjCHDH* interference and subsequent LPS exposure for 24 h. C: Representative TEM images of autophagy level of damaged mitochondria (arrowhead) in coelomocytes of *Apostichopus japonicus* after *AjCHDH* interference and subsequent *V. splendidus* infection for 24 h. D: Changes in ΔΨm in coelomocytes transfected with or without *AjCHDH* siRNA by JC-1 staining and flow cytometry. E: Changes in ΔΨm were determined after transfection with *AjCHDH* siRNA and subsequent LPS exposure for 24 h. **: $P<0.01$, $n=3$.

enhanced AjCHDH-LC3 association (Figure 4D), consistent with the results in Figure 4C.

AjCHDH knockdown impeded mitochondrial recruitment of SQSTM1 and LC3

To determine the effects of AjCHDH on the mitophagic function of SQSTM1 and LC3, we detected the mRNA expression levels of SQSTM1 and LC3 in coelomocytes transfected with *AjCHDH* siRNA, with no significant changes observed (Figure 5A, B). However, *AjCHDH* knockdown resulted in a significant reduction in the mitochondrial localization of SQSTM1 and LC3 (Figure 5C). Conversely, siRNA treatment induced a significant elevation in mitochondrial marker protein AjTim23, indicating that mitophagy was not activated and mitochondrial damage was exacerbated (Figure 5C). We further examined the mitochondrial colocalization of LC3 and SQSTM1 in control coelomocytes and *AjCHDH* knockdown cells using immunofluorescence staining. Confocal microscopy analysis revealed that the fluorescence intensity of SQSTM1 localized

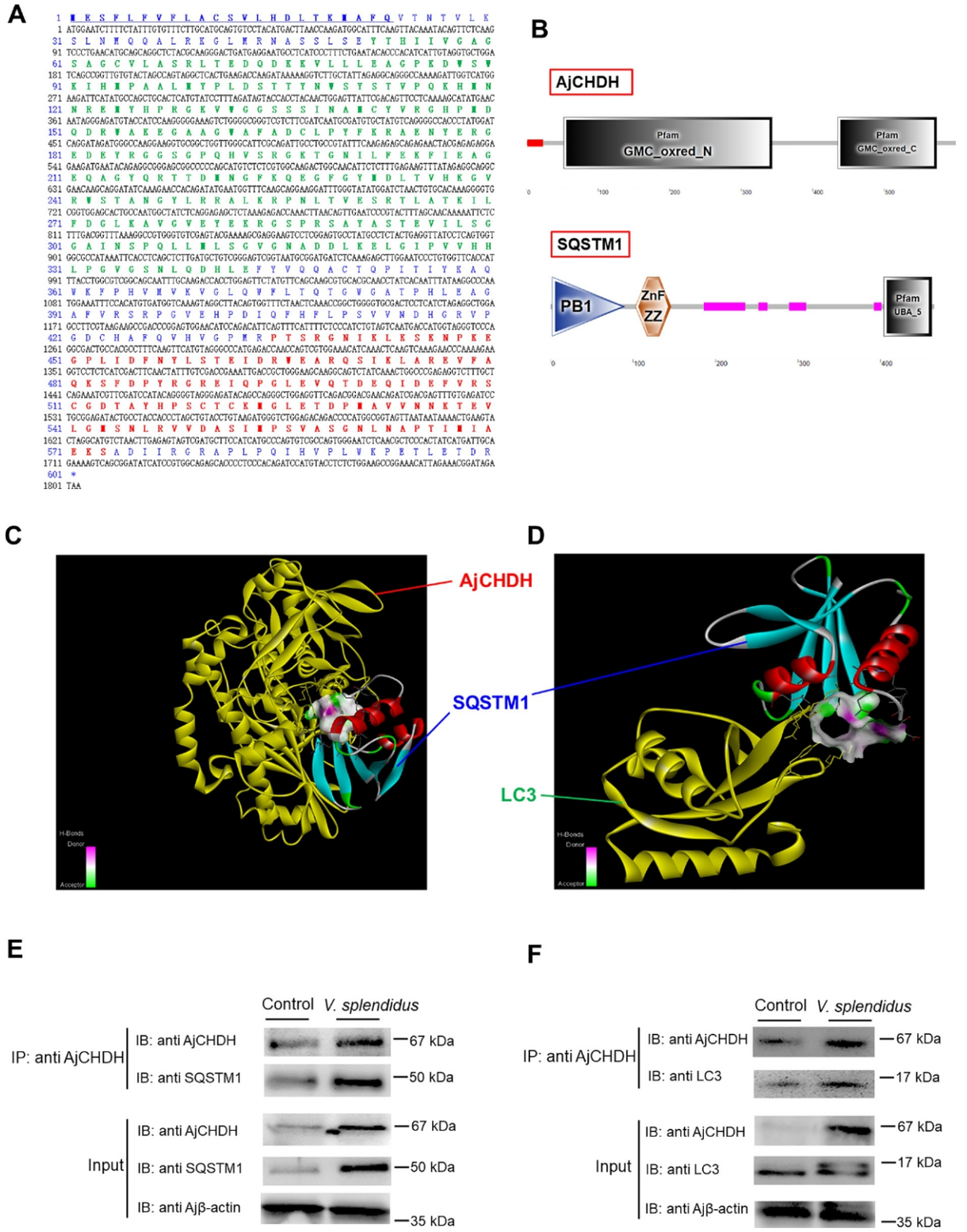

Figure 3 AjCHDH interacted with SQSTM1 to activate mitophagy

A: Amino acid (aa) sequence analysis of AjCHDH. Entire deduced aa sequence is depicted using single letter codes above corresponding nucleotide sequence. Signal peptide is underlined and indicated in bold. GMC_oxred_N is marked in green and indicated in bold. GMC_oxred_C domain is marked in red and indicated in bold. B: Predicted 2D structural model of AjCHDH and SQSTM1. C: Predicted combination model of AjCHDH and SQSTM1. D: Predicted combination model of SQSTM1 and LC3. E: AjCHDH was coimmunoprecipitated with SQSTM1 in coelomocytes. F: AjCHDH was coimmunoprecipitated with LC3 in coelomocytes.

to the mitochondria rapidly dissipated and aggregated to the puncta due to *AjCHDH* interference during mitophagy (Figure 5D). Furthermore, as depicted in Figure 5E, knockdown of *AjCHDH* significantly enhanced the aggregation of LC3 puncta and interrupted the colocalization of LC3 with mitochondria in *AjCHDH* siRNA-treated cells, confirming that AjCHDH is required for the recruitment of SQSTM1 and LC3 into mitochondria.

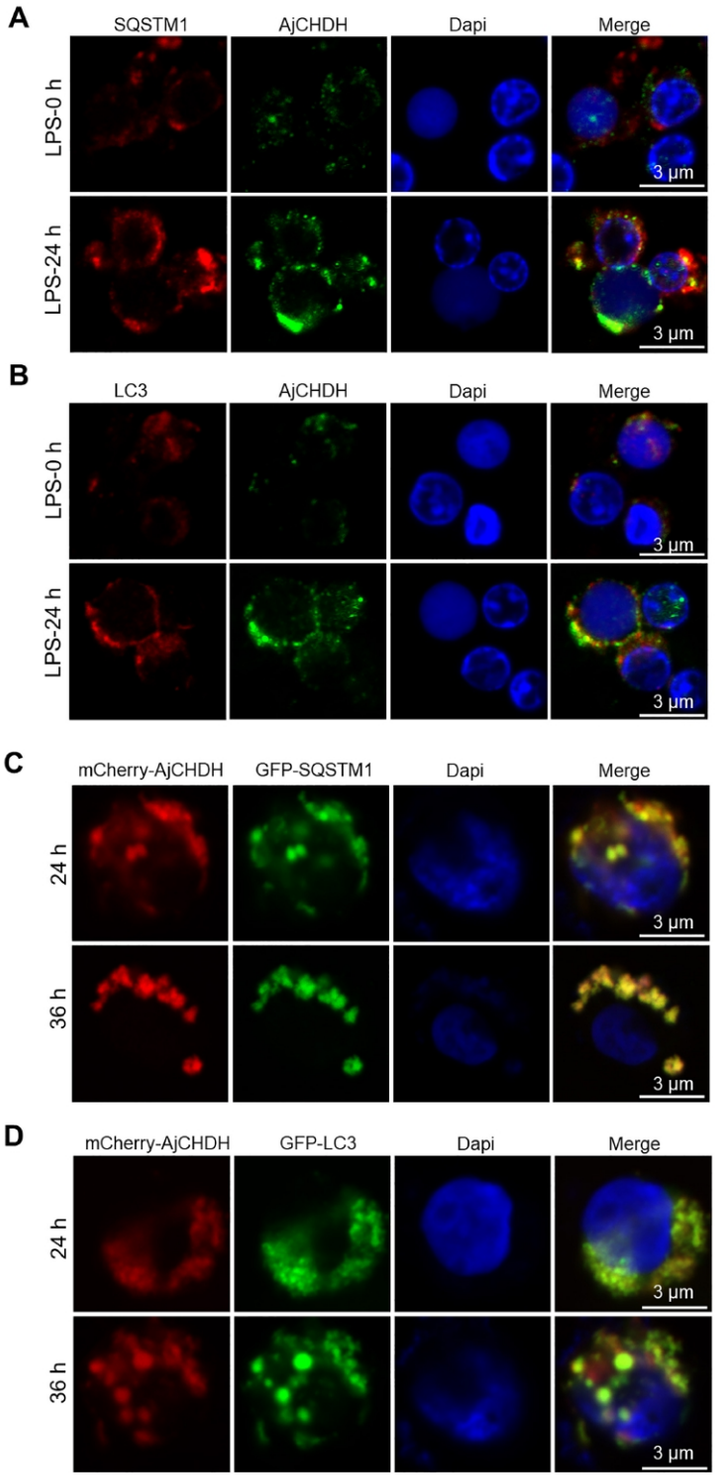

Figure 4 AjCHDH recruited SQSTM1 and LC3 during mitophagy

A: Immunofluorescence colocalization analysis of AjCHDH and SQSTM1 in coelomocytes after LPS treatment for 24 h, with DAPI (blue) staining to identify nuclei. B: Immunofluorescence colocalization analysis of AjCHDH and LC3 in coelomocytes after exposure to LPS for 24 h, with DAPI (blue) staining to identify nuclei. C: Immunofluorescence colocalization analysis of pCMV-N-Cherry-AjCHDH and pEGFP-N3-SQSTM1 in HEK293T cells after transfection for 24 and 36 h, with DAPI (blue) staining to identify nuclei. D: Co-transfection of pCMV-N-Cherry-AjCHDH, pCMV-Flag-2C-SQSTM1, and pIRES2-EGFP-LC3 in HEK293T cells for 24 and 36 h, with DAPI (blue) staining to identify nuclei.

AjCHDH-mediated mitophagy promoted ROS clearance and coelomocyte survival

In response to pathogen attack, mitochondria generate excessive ROS, which, in turn, impair mitochondrial function and induce apoptotic cell death (Youle & Van Der Bliek, 2012). Dysfunctional mitochondria must be selectively removed through mitophagy, a process controlled by several proteins (Li et al., 2021). Here, we investigated the function of AjCHDH-mediated mitophagy in mitigating ROS damage and apoptotic cell death at the cellular level in *A. japonicus*. As

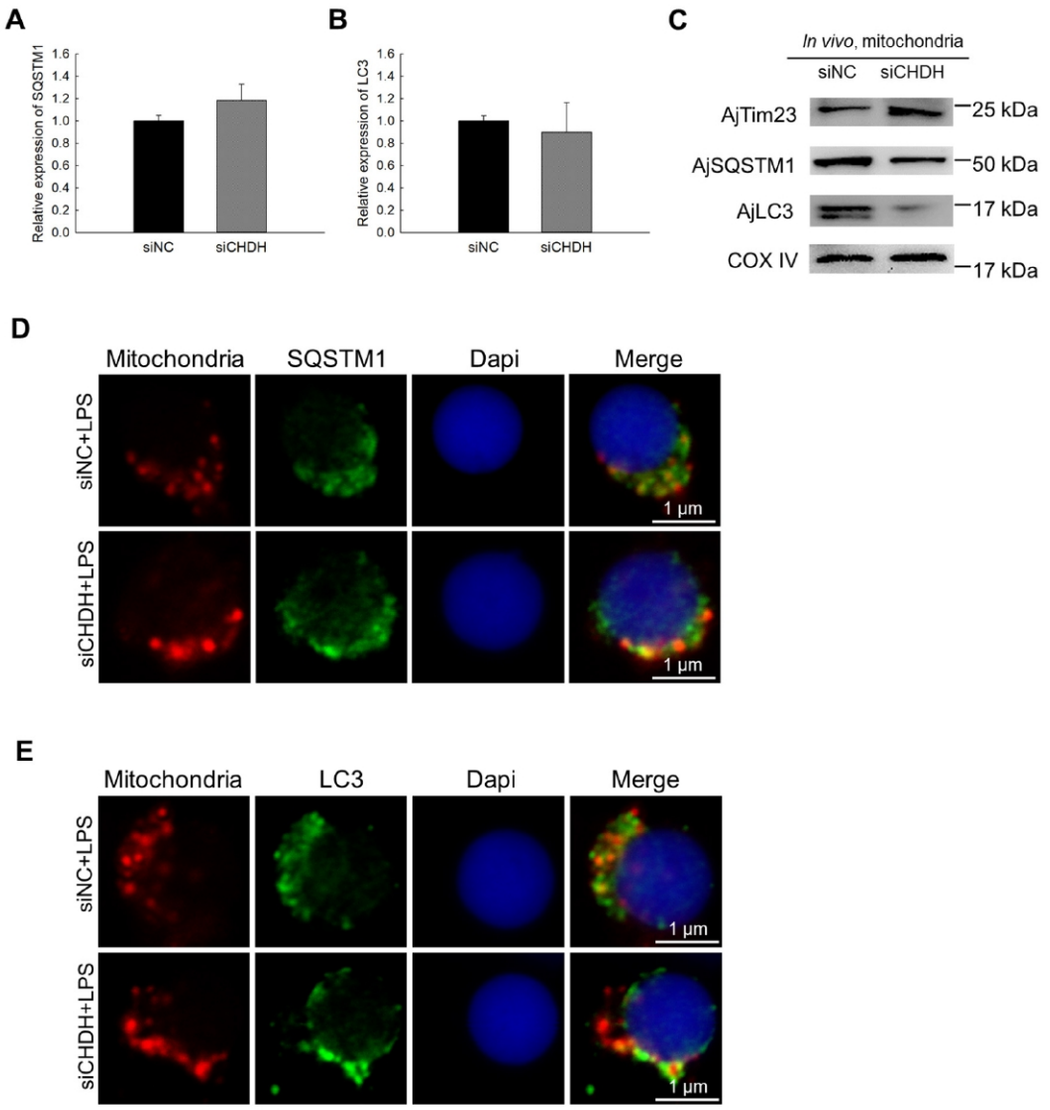

Figure 5 *AjCHDH* knockdown impeded recruitment of SQSTM1 and LC3 to mitochondria

A: mRNA levels of SQSTM1 in control coelomocytes and cells transfected with *AjCHDH* siRNA. *: $P<0.05$; **: $P<0.01$, $n=3$. B: mRNA levels of LC3 in control coelomocytes and cells transfected with *AjCHDH* siRNA. *: $P<0.05$; **: $P<0.01$, $n=3$. C: Protein levels of SQSTM1, LC3, and AjTim23 after transfection with or without *AjCHDH* siRNA. D: Immunofluorescence colocalization analysis of SQSTM1 in mitochondria after *AjCHDH* knockdown and treatment with LPS for 24 h, with DAPI (blue) staining to identify nuclei. E: Immunofluorescence colocalization analysis of LC3 in mitochondria after *AjCHDH* knockdown and treatment with LPS for 24 h, with DAPI (blue) staining to identify nuclei.

shown in Figure 6A, the level of mitochondrial ROS in coelomocytes significantly increased after *AjCHDH* interference. Additionally, intracellular ROS levels were also increased (1.27-fold, $P<0.05$) after coelomocytes were transfected with *AjCHDH* siRNA (Figure 6B, C). Importantly, *AjCHDH* interference triggered a significant increase in coelomocyte apoptosis (1.21-fold, $P<0.01$; Figure 6D, E) compared to the control group. Conversely, coelomocyte survival was significantly reduced (78%, $P<0.01$) in the *AjCHDH* knockdown group (Figure 6F).

DISCUSSION

Mitochondria play a crucial role in adenosine triphosphate (ATP) production and intracellular function but are also the primary source of ROS generation (Li et al., 2020; McBride et al., 2006). Dysfunctional or damaged mitochondria can lead to excessive ROS production from the electron transport chain, resulting in irreversible oxidative damage to the mitochondrial structure (Murphy et al., 2016). Failure to promptly eliminate these defective mitochondria can exacerbate ROS generation, resulting in increased peroxidation of mitochondrial components, oxidative stress, and ultimately, cell death (Mammucari & Rizzuto, 2010; Zorov et al., 2000). Therefore, maintaining mitochondrial homeostasis is vital for cellular functions. Mitophagy, a selective autophagy pathway that targets damaged mitochondria and eliminates excessive ROS through specific engulfment in lysosomes, is considered a critical cellular protective mechanism (Evans & Holzbaur, 2020). However, it remains unclear whether CHDH, a newly identified mitophagy receptor, can simultaneously recognize non-ubiquitinated SQSTM1 and LC3 to induce mitophagy in sea cucumbers. In this study, we identified AjCHDH, the CHDH protein from *A. japonicus*, and investigated its effects on mitophagy. Our findings demonstrated that AjCHDH was predominantly

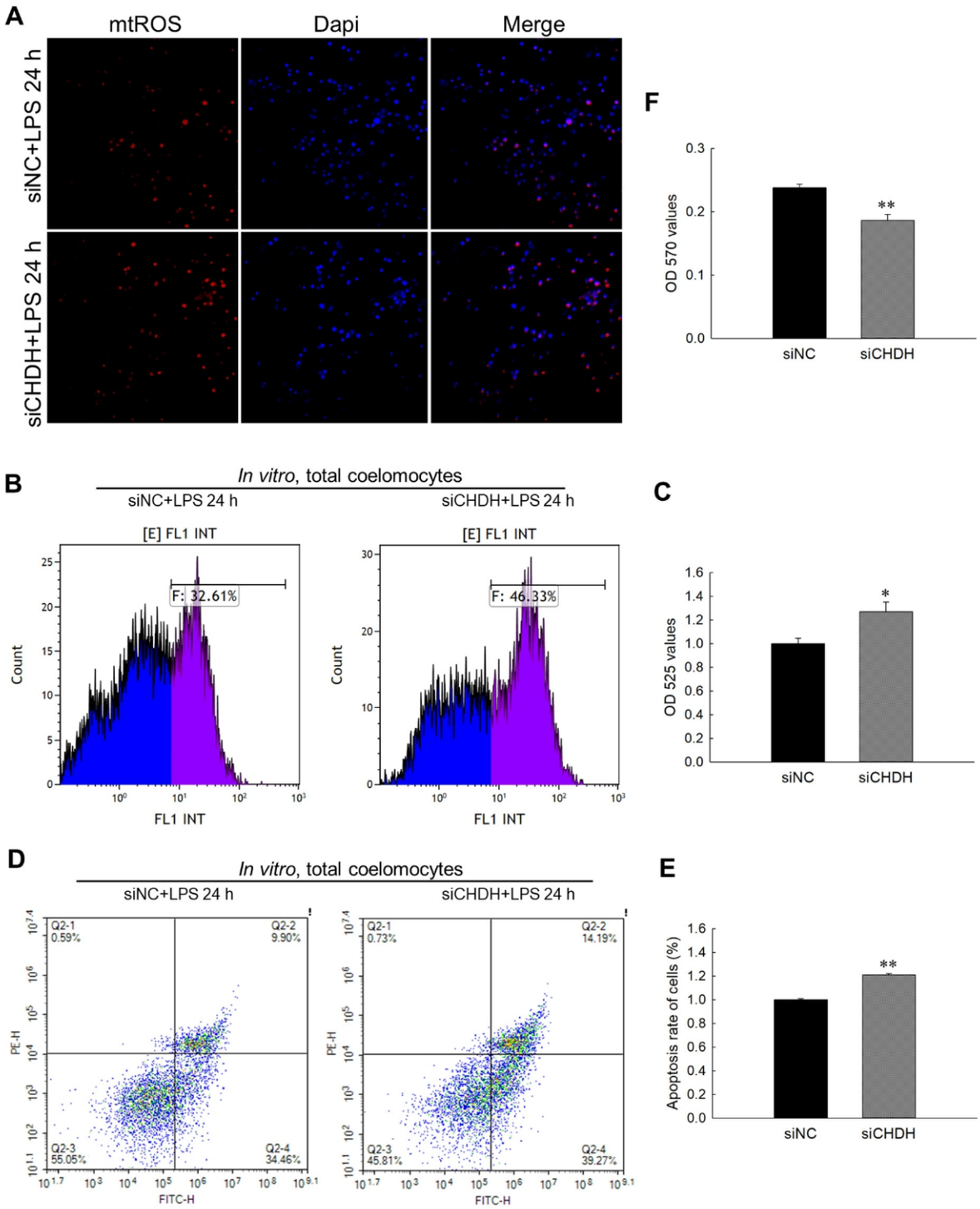

Figure 6 AjCHDH-mediated mitophagy promoted ROS clearance and coelomocyte survival

A: Mitochondrial ROS levels determined by MitoSOX staining after transfection with or without *AjCHDH* siRNA for 24 h. B: Representative images of intracellular ROS levels examined by DCFH-DA staining after transfection with or without *AjCHDH* siRNA for 24 h. C: Statistical analysis of changes in intracellular ROS levels from B. *: $P<0.05$, $n=3$. D: Representative images of apoptosis rate determined using an Annexin V-FITC/PI Apoptosis Assay Kit after transfection with *AjCHDH* siRNA and subsequent LPS exposure for 24 h. E: Statistical analysis of changes in apoptosis rate from D. **: $P<0.01$, $n=3$. F: Cell survival was determined after transfection with *AjCHDH* siRNA and subsequent LPS exposure for 24 h. **: $P<0.01$, $n=3$.

localized to the mitochondrial membrane of coelomocytes and played a pivotal role in mediating mitophagy (Figure 7). To the best of our knowledge, this is the first report of a mitophagy receptor in lower invertebrates that simultaneously recognizes non-ubiquitination damage signals and LC3.

Earlier studies on CHDH reported that it was located on the matrix side of the mitochondrial inner membrane and was involved in choline metabolism by catalyzing choline dehydrogenation to produce betaine aldehyde and release energy (De Ridder & Van Dam, 1973). However, recent research by Park et al. (2014) demonstrated that CHDH can be detected in both the mitochondrial inner and outer

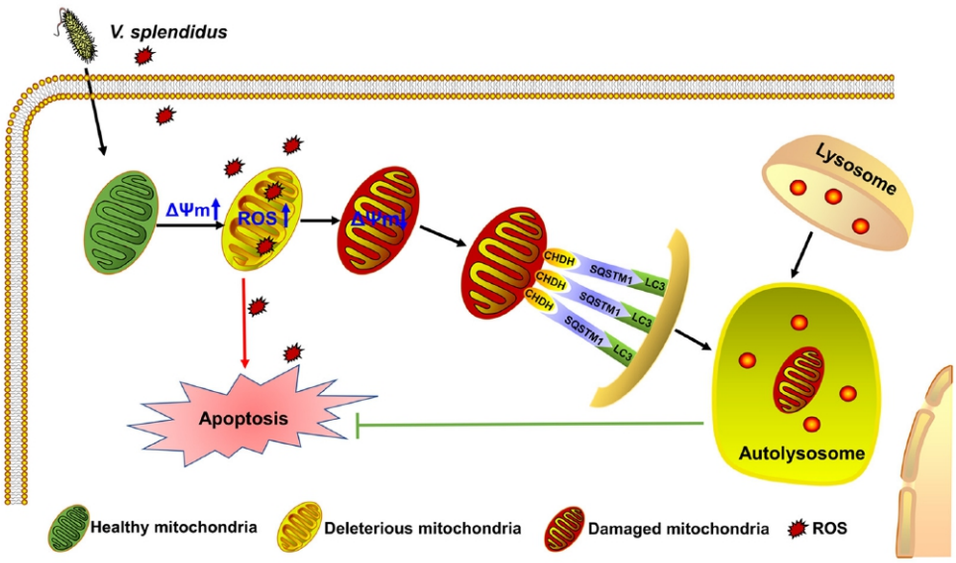

Figure 7 Role of AjCHDH-dependent mitophagy in *Vibrio splendidus* infection

Vibrio splendidus infection may induce an increase in mitochondrial membrane potential (ΔΨm) to generate ROS, which directly kill pathogens and trigger mitochondrial injury, thereby decreasing ΔΨm. To eradicate deleterious mitochondria and excessive ROS, mitochondrial receptor CHDH activates mitophagy by interacting with SQSTM1 and recruiting LC3.

membranes in resting cells. Interestingly, upon mitochondrial depolarization or damage, CHDH translocates and accumulates on the mitochondrial outer membrane to initiate mitophagy. Thus, the specific distribution of CHDH appears to be closely linked to its functionality. How does CHDH achieve translocation from the inner to outer membrane of mitochondria and perform different functions under these two conditions? Park et al. (2014) suggested that CHDH may exist in mitochondria as a transmembrane protein. Interestingly, Huang & Lin (2003) identified a putative 34 amino acid signal peptide at the N-terminus of the CHDH precursor sequence through comparison with the mature rat CHDH, which was later confirmed to be a transmembrane region. Notably, the N-terminal signal peptides not only facilitate accurate localization of CHDH in the mitochondria but also promote its translocation from the inner to outer mitochondrial membrane. In this study, we also found that AjCHDH contained a signal peptide sequence at the N-terminus (residues 1 to 23, Figure 3), indicating the presence of a mitochondrial targeting sequence, which provides a structural basis for exploring how CHDH initiates mitophagy in *A. japonicus*. The increased colocalization of AjCHDH with mitochondria after LPS challenge supports this notion. Additionally, the continuous increase in AjCHDH protein expression in the mitochondria, but not in the cytosol, following *V. splendidus* infection (Figure 1), further supports the involvement of AjCHDH in mitophagy.

Given its newfound role in mitophagy, understanding the location and regulatory mechanisms of CHDH is essential. In addition to the mitochondrial targeting sequence, previous research on the rat CHDH precursor has revealed the presence of multiple functional regions (Huang & Lin, 2003), consistent with our findings that AjCHDH contained a GMC domain in the N-terminus and a GMC oxidoreductase domain in the C-terminus. The C-terminal region is primarily responsible for binding the adenosine monophosphate (AMP) moiety of the FAD prosthetic group (Huang & Lin, 2003). Notably, Park et al. (2014) demonstrated that the FB1 domain in the N-terminal region of CHDH, which is exposed to the cytosol, plays a critical role in enabling the interaction between CHDH in damaged mitochondria and SQSTM1. Indeed, SQSTM1 is a key mitophagic adaptor that bridges depolarized mitochondria to autophagosomes (Li et al., 2014). While the ubiquitination of mitochondrial substrates by Parkin is critical in recruiting SQSTM1 to impaired mitochondria for degradation (Geisler et al., 2010; Lee et al., 2010; Narendra et al., 2010), increasing evidence has shown that SQSTM1 can interact with non-ubiquitinated substrates to activate mitophagy (Gal et al., 2009; Watanabe & Tanaka, 2011). In the current study, we observed interactions between AjCHDH and SQSTM1 in coelomocytes during *V. splendidus* infection based on coimmunoprecipitation and immunofluorescence staining. Moreover, the colocalization of AjCHDH with SQSTM1 in HEK293T cells confirmed that AjCHDH has an FB1 domain that interacts with SQSTM1. Additionally, Park et al. (2014) reported that overexpression of the FB1 domain in the cytosol can also bind to SQSTM1. Furthermore, mitophagy receptors require the recruitment of LC3 to ensure the encapsulation of damaged mitochondria by the isolation membrane or phagophore (Wei et al., 2015). Although a typical feature of mitophagy receptors is the presence of an LC3-interacting region (LIR), we found no LIR structural domain in AjCHDH. Thus, we speculate that when mitochondria lose their membrane potential, CHDH accumulates on the outer mitochondrial membrane, interacts with SQSTM1 via the FB1 domain, and recruits LC3 to form a ternary protein complex, thereby inducing mitophagy in damaged mitochondria. As shown in Figure 4, colocalization of AjCHDH and LC3 was observed in both coelomocytes and HEK293T cells. Furthermore, the protein levels of SQSTM1 and LC3 recruited to the mitochondria were both significantly reduced after *AjCHDH* knockdown (Figure 5), indicating that AjCHDH is involved in the regulation of mitophagy in the coelomocytes of *A. japonicus*.

How is mitophagy activated, and what is the significance of its occurrence? Recent studies have suggested that ROS play a critical role in regulating mitophagy, potentially serving as a trigger for mitophagy (Volpe et al., 2018; Zhang et al., 2019).

While mitochondria are the primary sites of ROS generation, excessive ROS accumulation can impair mitochondrial membrane potential, leading to irreversible oxidative damage and cell death (Huang et al., 2019; Murphy et al., 2016; Orrenius et al., 2007; Wang et al., 2020). However, a reduction in membrane potential can also lead to the recruitment of mitochondrial receptors, which can combine with autophagy adapters and LC3 to activate mitophagy (Pavón et al., 2019). Although most studies on the regulatory mechanisms of mitophagy have focused on the PINK1-PRKN pathway, emerging evidence suggests that this pathway is not the sole mechanism, and mitophagy can still occur in the absence of parkin (Villa et al., 2018). Considering the absence of the PINK1-PRKN regulatory axis in our study species, *A. japonicus*, we endeavored to investigate alternative mechanisms for triggering mitophagy. Our study revealed that knockdown of the AjCHDH receptor in coelomocytes led to a significant decrease in mitophagy levels (Figure 2). This is consistent with the results of Park et al. (2014), which showed that *CHDH* knockdown can inhibit mitophagy, while overexpression of CHDH promotes mitophagy. These findings underscore the crucial role of AjCHDH in initiating mitophagy in *A. japonicus*. Additionally, we demonstrated that *AjCHDH* interference blocked the clearance and renewal of dysfunctional mitochondria, as evidenced by the low mitochondrial membrane potential after *AjCHDH* knockdown. Mitophagy also functions more broadly, including the maintenance of mitochondrial homeostasis, mitigation of ROS damage, and promotion of cell survival (Bhatia-Kiššová & Camougrand, 2013; Wang & Zhou, 2020). Defective mitophagy can exacerbate damaged mitochondria and ROS accumulation, leading to diverse pathophysiological diseases (Choi, 2020; Fivenson et al., 2017; Gong et al., 2015). Consistently, our results suggested that AjCHDH-mediated mitophagy plays a protective role in LPS-induced coelomocyte death, as evidenced by the increase in ROS and apoptosis following *AjCHDH* interference (Figure 6). Furthermore, to demonstrate that AjCHDH is an indispensable mitophagy receptor, we depleted *AjCHDH* using siRNA and found that *AjCHDH* knockdown significantly impaired coelomocyte survival. These results are in line with the recent findings of Ashrafi & Schwarz (2013) and Pal et al. (2022) showing a functional link between mitophagy and cell survival. Insights provided by Chang et al. (2021, 2022) have also shed light on the key role of mitophagy in coronary endothelial cells and microvascular dysfunction in myocardial infarction and ischemic cardiomyopathy, highlighting the potential of targeting mitochondrial quality control as a novel therapeutic approach. In this study, we clarified the physiological importance of mitophagy in maintaining mitochondrial quality and promoting coelomocyte survival in *A. japonicus*. Impairment in AjCHDH-dependent mitophagy can lead to damaged mitochondria and ROS accumulation, resulting in increased cell death. These results indicate that AjCHDH-mediated mitophagy is required for maintaining mitochondrial homeostasis, and that AjCHDH may be a promising therapeutic target for diseases induced by excessive ROS by regulating damaged mitophagy.

SUPPLEMENTARY DATA

Supplementary data to this article can be found online.

COMPETING INTERESTS

The authors declare that they have no competing interests.

AUTHORS' CONTRIBUTIONS

L.L.S. conducted the experiments, processed the data, and wrote the manuscript; Y.F.D. and C.H.L. participated in the experimental design and revised the manuscript. M.X.Y. and C.H.L. contributed new reagents and analytic tools. All authors read and approved the final version of the manuscript.

ACKNOWLEDGMENTS

The authors thank Dr. Yan-Zhen Tian for help in confocal laser microscopy.

REFERENCES

Apel K, Hirt H. 2004. Reactive oxygen species: metabolism, oxidative stress, and signal transduction. *Annual Review of Plant Biology*, **55**: 373−399.

Ashrafi G, Schwarz TL. 2013. The pathways of mitophagy for quality control and clearance of mitochondria. *Cell Death & Differentiation*, **20**(1): 31−42.

Bao DK, Zhao J, Zhou XC, et al. 2019. Mitochondrial fission-induced mtDNA stress promotes tumor-associated macrophage infiltration and HCC progression. *Oncogene*, **38**(25): 5007−5020.

Barnham KJ, Masters CL, Bush AI. 2004. Neurodegenerative diseases and oxidative stress. *Nature Reviews Drug Discovery*, **3**(3): 205−214.

Bhatia-Kiššová I, Camougrand N. 2013. Mitophagy: a process that adapts to the cell physiology. *The International Journal of Biochemistry & Cell Biology*, **45**(1): 30−33.

Chang X, Lochner A, Wang HH, et al. 2021. Coronary microvascular injury in myocardial infarction: perception and knowledge for mitochondrial quality control. *Theranostics*, **11**(14): 6766−6785.

Chang X, Toan S, Li RB, et al. 2022. Therapeutic strategies in ischemic cardiomyopathy: focus on mitochondrial quality surveillance. *eBioMedicine*, **84**: 104260.

Choi ME. 2020. Autophagy in kidney disease. *Annual Review of Physiology*, **82**: 297−322.

De Ridder JJM, Van Dam K. 1973. The efflux of betaine from rat-liver mitochondria, a possible regulating step in choline oxidation. *Biochimica et Biophysica Acta (BBA) - Biomembranes*, **291**(2): 557−563.

Deng H, He CB, Zhou ZC, et al. 2008. Isolation and pathogenicity of pathogens from skin ulceration and viscera ejection syndrome of sea cucumber. *Journal of Biotechnology*, **136**(S1): S551.

Ding WX, Ni HM, Li M, et al. 2010. Nix is critical to two distinct phases of mitophagy, reactive oxygen species-mediated autophagy induction and Parkin-ubiquitin-p62-mediated mitochondrial priming. *Journal of Biological Chemistry*, **285**(36): 27879−27890.

Elmore SP, Qian T, Grissom SF, et al. 2001. The mitochondrial permeability transition initiates autophagy in rat hepatocytes. *The FASEB Journal*, **15**(12): 1−17.

Evans CS, Holzbaur EL. 2020. Degradation of engulfed mitochondria is rate-limiting in optineurin-mediated mitophagy in neurons. *eLife*, **9**: e50260.

Fivenson EM, Lautrup S, Sun N, et al. 2017. Mitophagy in neurodegeneration and aging. *Neurochemistry International*, **109**: 202−209.

Gal J, Ström AL, Kwinter DM, et al. 2009. Sequestosome 1/p62 links familial ALS mutant SOD1 to LC3 via an ubiquitin-independent mechanism. *Journal of Neurochemistry*, **111**(4): 1062−1073.

Geisler S, Holmström KM, Skujat D, et al. 2010. PINK1/Parkin-mediated mitophagy is dependent on VDAC1 and p62/SQSTM1. *Nature Cell Biology*, **12**(2): 119−131.

Gong GH, Song MS, Csordas G, et al. 2015. Parkin-mediated mitophagy directs perinatal cardiac metabolic maturation in mice. *Science*, **350**(6265): aad2459.

Howard S, Bottino C, Brooke S, et al. 2002. Neuroprotective effects of bcl-2 overexpression in hippocampal cultures: interactions with pathways of oxidative damage. *Journal of Neurochemistry*, **83**(4): 914−923.

Huang HL, Ullah F, Zhou DX, et al. 2019. Mechanisms of ROS regulation of plant development and stress responses. *Frontiers in Plant Science*, **10**: 800.

Huang SB, Lin QS. 2003. Functional expression and processing of rat choline dehydrogenase precursor. *Biochemical and Biophysical Research Communications*, **309**(2): 344−350.

Jin SM, Youle RJ. 2012. PINK1- and Parkin-mediated mitophagy at a glance. *Journal of Cell Science*, **125**(Pt 4): 795–799.

Lee JY, Nagano Y, Taylor JP, et al. 2010. Disease-causing mutations in parkin impair mitochondrial ubiquitination, aggregation, and HDAC6-dependent mitophagy. *Journal of Cell Biology*, **189**(4): 671−679.

Li AQ, Gao M, Jiang WT, et al. 2020. Mitochondrial dynamics in adult cardiomyocytes and heart diseases. *Frontiers in Cell and Developmental Biology*, **8**: 584800.

Li Y, Wang SG, Ni HM, et al. 2014. Autophagy in alcohol-induced multiorgan injury: mechanisms and potential therapeutic targets. *BioMed Research International*, **2014**: 498491.

Li Y, Zheng WQ, Lu YY, et al. 2021. BNIP3L/NIX-mediated mitophagy: molecular mechanisms and implications for human disease. *Cell Death & Disease*, **13**(1): 14.

Lin CS, Wu RD. 1986. Choline oxidation and choline dehydrogenase. *Journal of Protein Chemistry*, **5**(3): 193−200.

Liu HZ, Zheng FR, Sun XQ, et al. 2010. Identification of the pathogens associated with skin ulceration and peristome tumescence in cultured sea cucumbers *Apostichopus japonicus* (Selenka). *Journal of Invertebrate Pathology*, **105**(3): 236−242.

Liu L, Sakakibara K, Chen Q, et al. 2014. Receptor-mediated mitophagy in yeast and mammalian systems. *Cell Research*, **24**(7): 787−795.

Livak KJ, Schmittgen TD. 2001. Analysis of relative gene expression data using real-time quantitative PCR and the $2^{-\Delta\Delta CT}$ method. *Methods*, **25**(4): 402−408.

Luo J, Mills K, Le Cessie S, et al. 2020. Ageing, age-related diseases and oxidative stress: what to do next. *Ageing Research Reviews*, **57**: 100982.

Ma YX, Xu GR, Chang YQ, et al. 2006. Bacterial pathogens of skin ulceration disease in cultured sea cucumber *Apostichopus japonicus* (Selenka) juveniles. *Journal of Dalian Fisheries University*, **21**(1): 13−18. (in Chinese)

Mammucari C, Rizzuto R. 2010. Signaling pathways in mitochondrial dysfunction and aging. *Mechanisms of Ageing and Development*, **131**(7–8): 536–543.

McBride HM, Neuspiel M, Wasiak S. 2006. Mitochondria: more than just a powerhouse. *Current Biology*, **16**(14): R551−R560.

Métivier D, Dallaporta B, Zamzami N, et al. 1998. Cytofluorometric detection of mitochondrial alterations in early CD95/Fas/APO-1-triggered apoptosis of Jurkat T lymphoma cells. Comparison of seven mitochondrion-specific fluorochromes. *Immunology Letters*, **61**(2–3): 157–163.

Murphy E, Ardehali H, Balaban RS, et al. 2016. Mitochondrial function, biology, and role in disease. *Circulation Research*, **118**(12): 1960−1991.

Narendra D, Kane LA, Hauser DN, et al. 2010. p62/SQSTM1 is required for Parkin-induced mitochondrial clustering but not mitophagy; VDAC1 is dispensable for both. *Autophagy*, **6**(8): 1090−1106.

Nguyen TN, Padman BS, Lazarou M. 2016. Deciphering the molecular signals of PINK1/Parkin mitophagy. *Trends in Cell Biology*, **26**(10): 733−744.

Nunnari J, Suomalainen A. 2012. Mitochondria: in sickness and in health. *Cell*, **148**(6): 1145−1159.

Orrenius S, Gogvadze V, Zhivotovsky B. 2007. Mitochondrial oxidative stress: implications for cell death. *Annual Review of Pharmacology and Toxicology*, **47**: 143−183.

Pal A, Paripati AK, Deolal P, et al. 2022. Eisosome protein Pil1 regulates mitochondrial morphology, mitophagy, and cell death in *Saccharomyces cerevisiae*. *Journal of Biological Chemistry*, **298**(11): 102533.

Pankiv S, Clausen TH, Lamark T, et al. 2007. p62/SQSTM1 binds directly to Atg8/LC3 to facilitate degradation of ubiquitinated protein aggregates by autophagy. *Journal of Biological Chemistry*, **282**(33): 24131−24145.

Park S, Choi SG, Yoo SM, et al. 2014. Choline dehydrogenase interacts with SQSTM1/p62 to recruit LC3 and stimulate mitophagy. *Autophagy*, **10**(11): 1906−1920.

Pavón N, Buelna-Chontal M, Macías-López A, et al. 2019. On the oxidative damage by cadmium to kidney mitochondrial functions. *Biochemistry and Cell Biology*, **97**(2): 187−192.

Sun LL, Guo M, Lv ZM, et al. 2020. Hypoxia-inducible factor-1α shifts metabolism from oxidative phosphorylation to glycolysis in response to pathogen challenge in *Apostichopus japonicus*. *Aquaculture*, **526**: 735393.

Sun LL, Shao YN, You MX, et al. 2022. ROS-mediated BNIP3-dependent mitophagy promotes coelomocyte survival in *Apostichopus japonicus* in response to *Vibrio splendidus* infection. *Zoological Research*, **43**(2): 285−300.

Tolkovsky AM. 2009. Mitophagy. *Biochimica et Biophysica Acta (BBA) - Molecular Cell Research*, **1793**(9): 1508−1515.

Villa E, Marchetti S, Ricci JE. 2018. No parkin zone: mitophagy without parkin. *Trends in Cell Biology*, **28**(11): 882−895.

Volpe CMO, Villar-Delfino PH, Dos Anjos PMF, et al. 2018. Cellular death, reactive oxygen species (ROS) and diabetic complications. *Cell Death & Disease*, **9**(2): 119.

Wang J, Toan S, Zhou H. 2020. New insights into the role of mitochondria in cardiac microvascular ischemia/reperfusion injury. *Angiogenesis*, **23**(3): 299−314.

Wang J, Zhou H. 2020. Mitochondrial quality control mechanisms as molecular targets in cardiac ischemia–reperfusion injury. *Acta Pharmaceutica Sinica B*, **10**(10): 1866−1879.

Watanabe Y, Tanaka M. 2011. p62/SQSTM1 in autophagic clearance of a non-ubiquitylated substrate. *Journal of Cell Science*, **124**(16): 2692−2701.

Wei HF, Liu L, Chen Q. 2015. Selective removal of mitochondria via mitophagy: distinct pathways for different mitochondrial stresses. *Biochimica et Biophysica Acta (BBA) - Molecular Cell Research*, **1853**(10): 2784−2790.

West AP, Brodsky IE, Rahner C, et al. 2011. TLR signalling augments macrophage bactericidal activity through mitochondrial ROS. *Nature*, **472**(7344): 476−480.

Yamano K, Matsuda N, Tanaka K. 2016. The ubiquitin signal and autophagy: an orchestrated dance leading to mitochondrial degradation. *EMBO Reports*, **17**(3): 300−316.

Yoo SM, Jung YK. 2018. A molecular approach to mitophagy and mitochondrial dynamics. *Molecules and Cells*, **41**(1): 18−26.

Youle RJ, Van Der Bliek AM. 2012. Mitochondrial fission, fusion, and stress. *Science*, **337**(6098): 1062−1065.

Zeb A, Choubey V, Gupta R, et al. 2021. A novel role of KEAP1/PGAM5 complex: ROS sensor for inducing mitophagy. *Redox Biology*, **48**: 102186.

Zhang PJ, Li CH, Shao YN, et al. 2014. Identification and characterization of miR-92a and its targets modulating *Vibrio splendidus* challenged *Apostichopus japonicus*. *Fish & Shellfish Immunology*, **38**(2): 383–388.

Zhang YP, Xi XT, Mei Y, et al. 2019. High-glucose induces retinal pigment epithelium mitochondrial pathways of apoptosis and inhibits mitophagy by regulating ROS/PINK1/Parkin signal pathway. *Biomedicine & Pharmacotherapy*, **111**: 1315−1325.

Zorov DB, Filburn CR, Klotz LO, et al. 2000. Reactive oxygen species (ROS)-induced ROS release: a new phenomenon accompanying induction of the mitochondrial permeability transition in cardiac myocytes. *The Journal of Experimental Medicine*, **192**(7): 1001−1014.